IEEE Transactions on Industrial Electronics, Available online 16 June 2026
DOI: 10.1109/tie.2026.3695234

Benchmarking the Engineering Reliability of LLM Based Design for Resonant Wireless Power Transfer Systems

Khalifa Aliyu Ibrahim, *Member*, Patrick Chi-Kwong Luk, *Senior Member, IEEE*, Zhenhua Luo, Seng Yim Ng, Lee Harrison

***Abstract*— Designing high frequency wireless power transfer (WPT) systems is a complex process that demands considerable time and domain expertise. To address these challenges, this study employs both general purpose and finetuned large language model (LLM) agents to automate the WPT design process. The finetuned models embed WPT domain specific knowledge using instructions capable of generating complete coil and circuit level parameters including geometry, conductor type, compensation values, and frequency targets within seconds. Among the tested agents, High Frequency Power Electronics (HFPE-4o) achieved the best performance, reducing design time by a factor of 120 (representing a 99.17% reduction compared with conventional methods). The generated design achieved 99.98% accuracy, successfully producing all required parameters without additional input. Validation through PSIM and ANSYS simulations confirmed electromagnetic and circuit level accuracy, while 150W experimental results verified system operation at 85 kHz with less than 8% deviation from predictions. Comparative evaluation against general purpose models such as ChatGPT-5 further demonstrated the advantage of domain adaptation, revealing significant improvements in numerical reliability and design stability. These findings confirm that LLM driven workflows can accelerate WPT system design while preserving engineering precision. By establishing a foundation for iterative refinement, the proposed AI-driven agentic framework provides a promising pathway for integrating intelligent LLM agents into next generation power electronics design workflows.**

***Index Terms* — Large Language Models (LLMs), artificial intelligent assisted design, high frequency resonant wireless power transfer (WPT), power electronics, electromagnetic simulation, experimental validation, coil design.**

I. Introduction

The improvement of electrical systems remains a core component of global energy strategies [1]. With increasing demand for energy efficient technologies. Recent advancement in artificial intelligent (AI) have emerged as a promising solution to enhance power electronic design as reported in many recent studies [2], [3], [4], [5]. High frequency wireless power transfer (HFWPT) technology has emerged as a promising approach [6], [7], [8], where physical connectors are impractical or undesirable. However, the conventional design process for power electronics (PE) systems including wireless power transfer (WPT) is often complex, resource intensive, and time consuming [9], [10]. This traditional process typically involves multiple stages such as conceptualization, design specification, mathematical modeling, simulation, optimization, prototyping, and testing. Each of these phases requires precise engineering calculations and expert judgment, making the process vulnerable to human error and inefficiencies.

As demand grows for smarter, faster, and more reliable power electronics (PE) systems, there is a pressing need to rethink the design process itself [11]. Streamlining this process can lead to significant reductions in development time and cost, while also improving performance, reliability, and scalability. Recent efforts in power electronics research have leveraged computational tools and machine learning to support specific stages of the design process, as reported in [12], [13], [14], [15]. For example, neural networks, genetic algorithms and particle swarm optimization have been applied to parameter optimization [16], and machine learning techniques have been explored for automatic circuit layout generation. However, most existing approaches remain limited in scope and typically address only isolated stages of the design process. As a result, they do not fully exploit recent advances in artificial intelligence for integrated end to end design automation. In particular, the rapid progress in generative artificial intelligence and large language models has not yet been systematically explored for wireless power transfer system design. Existing studies largely overlook the potential of large language models to provide context aware and multistage design support spanning conceptualization, analytical modelling, simulation, and hardware realization. The purpose of the present work is to evaluate whether large language models can autonomously generate complete, physically feasible wireless power transfer designs from engineering specifications, rather than to benchmark all artificial intelligence based optimization methods. Consequently, a critical gap remains in methodologies

This work was sponsored by QBYSS, Cranfield University United Kingdom. *Corresponding author:* Patrick Chi-Kwong Luk.

Khalifa Aliyu Ibrahim is with Energy and Power, Cranfield University, Cranfield MK43 0AL, U.K (Khalifa-Aliyu.Ibrahim@cranfield.ac.uk).

Patrick Chi-Kwong Luk is with Energy and Power, Cranfield University, Cranfield MK43 0AL, U.K. (p.c.k.luk@cranfield.ac.uk).

Zhenhua Luo is with Energy Storage and Harvesting Centre for Energy Engineering at Cranfield University, Cranfield MK43 0AL, U.K. (Z.Luo@cranfield.ac.uk).

Seng Yim Ng is with SYNG Power Consulting Ltd, 78 High Street, Newport Pagnell, England, MK16 8AQ, UK. (sengyim.ng@syngpowerconsultingltd.com)

Lee Harrison is with QBYSS, Unit 28/29 Innovation Centre, University Way, Cranfield Technology Park, Bedfordshire, MK43 0BT, UK. (lee.harrison@QBYSS.com)

This submission provided the LLM agent instructions, and pseudocode of the design workflow in the GitHub repository, while video recordings of each agent's design generation process as supplementary document.

Published by IEEE. This is the Author Accepted Manuscript issued with: Creative Commons Attribution License (CC:BY 4.0).
The final published version (version of record) is available online at DOI:10.1109/tie.2026.3695234. Please refer to any applicable publisher terms of use.

that enable autonomous end to end wireless power transfer system design with quantitative evaluation of design correctness and reliability. To the best of the authors' knowledge, this work presents the first benchmarking framework that evaluates the correctness, completeness, and numerical reliability of large language model generated power electronics designs with experimental validation.

To address this gap, this paper builds upon our previous feasibility study in [4], which introduced an initial LLM assisted design framework. Unlike [4], which did not employ an agentic design strategy and did not include electromagnetic simulation, hardware fabrication, or overload analysis, the present work significantly extends the framework into a fully agentic, quantitatively benchmarked, and experimentally validated design methodology. Specifically, this study introduces a multi agent LLM design approach, integrates ANSYS based electromagnetic field simulation, and demonstrates physical coil fabrication and experimental testing of an LLM designed WPT system. The primary objective of this work is not to optimize WPT efficiency, but to rigorously evaluate whether large language models can autonomously generate complete, physically feasible, and experimentally realizable designs, and to establish a quantitative benchmarking framework for assessing their engineering reliability. The key contributions of this paper are as follows:

I. First agentic LLM based benchmarking framework for PE design, enabling autonomous multi-agent generation and evaluation of WPT coil and circuit parameters.
II. Introduction of quantitative correctness and strict completeness metrics for objective assessment of LLM generated designs against analytical baselines.
III. Multi agent evaluation of seven finetuned LLMs and one general-purpose model, exposing performance variability, failure modes, and domain specific limitations in high frequency PE design.
IV. First electromagnetic validation and experimental fabrication of an LLM-generated WPT coil using ANSYS FEM analysis and hardware testing.
V. Overload-induced failure analysis of the LLM designed system, providing insight into robustness, thermal limits, and real-world feasibility.
VI. Demonstration of a design time reduction exceeding two orders of magnitude relative to conventional manual workflows.

The remainder of this paper is organized as follows. Section II introduces the proposed LLM driven agentic design methodology. Section III presents the LLM based design process, analytical modeling, simulation approach, and experimental setup. Section IV discusses the results and benchmarking outcomes. Section V provides a discussion on limitations, generalizability, and future research directions. Section VI concludes the paper.

II. Proposed LLM Methodology

This paper presents a design case study of a WPT system using an AI-assisted framework based on OpenAI's LLMs. The entire system is designed using a finetuned custom LLM-AI platform, termed High Frequency Power Electronics AI (HFPE.AI), comprising seven generative pretrained transformer (GPT) agents and a general purpose ChatGPT-5 model. Fig. 1 presents the complete pipeline of the proposed LLM-driven design automation framework for high frequency WPT systems. The process begins with a structured design prompt, which includes inputs such as Objective and Conceptual Design (O&CD), Specification and Requirements (SP/R), and the target power transfer efficiency (η). The most promising designs are further validated using ANSYS 3D finite element electromagnetic simulations and PSIM circuit level simulations. Finally, the selected design is fabricated and experimentally tested to demonstrate the feasibility, robustness, and limitations of the LLM-driven design approach.

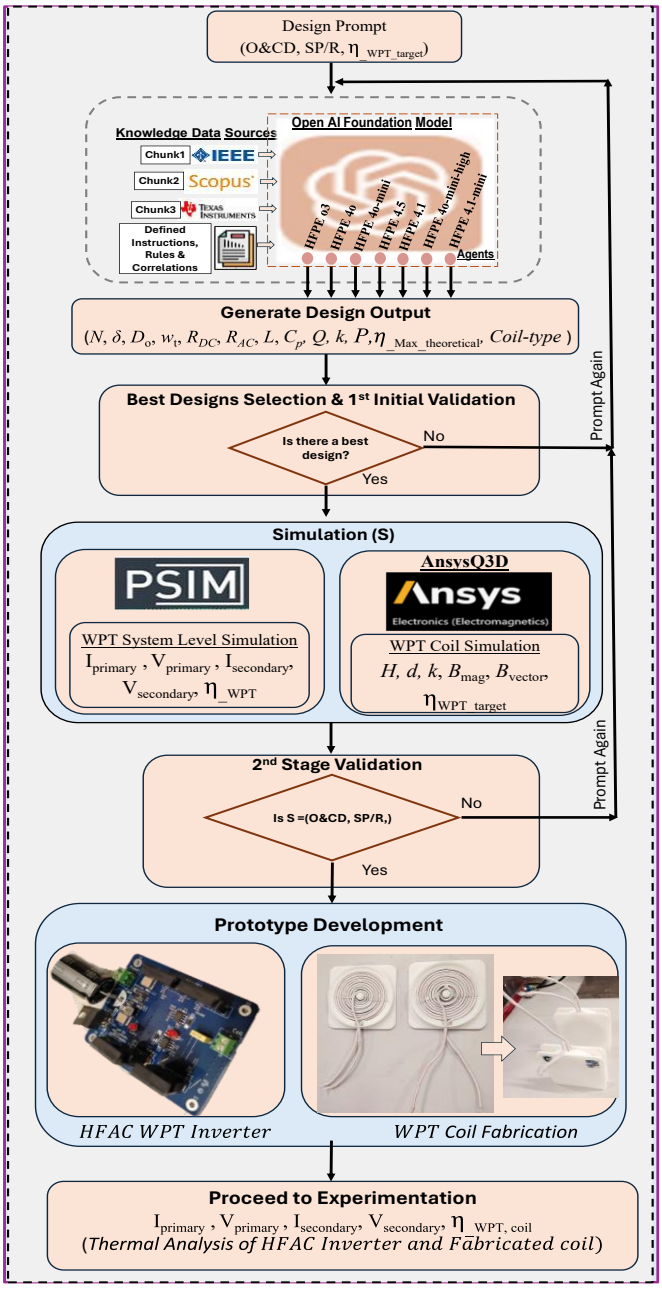


Fig. 1. Design workflow of LLMs AI for WPT design.

In this work, the term context finetuning refers to domain specific instruction tuning and constrained prompt engineering, rather than retraining or modifying the underlying foundation model weights. These GPT agents leverage the OpenAI foundation model and are augmented with WPT domain specific knowledge data from domain research paper available IEEE, Scopus, Texas Instruments datasheets, and similar technical sources to enhance their design capabilities. A total of 3000 pages of data was used for the context finetuning knowledge. Each agent variant such as HFPE-4o, HFPE-o3, HFPE-4o-mini, HFPE-4o-mini-high, HFPE-4.5, HFPE-4.1, and HFPE-4.1-mini are referred to as a distinct LLM agent, representing a unique configuration in terms of language capabilities, design response behavior, and computational efficiency.

The agents generate full WPT designs output, including electrical and geometric parameters like the number of turns (N), skin depth (δ), outer diameter D_o (Do), wire thickness w_t, DC resistance R_{DC}, AC resistance R, inductance (L), parasitic capacitance C_p, coupling coefficient (k), and theoretical maximum efficiency (η),along with a suitable coil type. If no satisfactory design is produced, a new prompt can be given again. Once a viable candidate is selected, simulation is conducted in two domains. PSIM version 3.0.60 for system level simulation (voltage, current, power and efficiency), and ANSYS Q3D Electronics Suite 2021-R2 for electromagnetic coil simulation (magnetic flux density B, field strength H, and coupling behavior). If simulation results do not satisfy the original design constraints (O&CD, SP/R), another prompt can be reinitiated. Otherwise, the design proceeds to prototype development, involving both high frequency alternating current (HFAC) inverter assembly and WPT coil fabrication. The final stage is experimental validation, where key performance metrics such as current, voltage, efficiency and operation condition are measured to assess electrical performance and thermal behavior. This framework unifies computation and mathematical modelling (C/MM), keep the design information that could be useful for component Selection (CS), coding and schematic design (C/SD), and sets the foundation for future Certification and Compliance (CC), enabling an end to end automated design to prototype flow for modern WPT system.

A. LLM Prompt Design And Evaluation Metrics

Fig. 2 presents the structured prompt framework developed to guide the LLM in generating WPT designs. The prompt activates domain-specific expertise ("fine-tuned LLM model specialized in Wireless Power Transfer"), defines a precise design objective ("design a WPT with a high efficiency resonant inductive coil"), and specifies full technical constraints including operating frequency, wire limitations, and target efficiency. It enforces a step by step methodology and mandates computation of the complete parameter set skin depth (δ), R_{DC}, R, L, Cp, C, Q, and η_{max} while prescribing exact design inputs such as coupling coefficient and Litz wire configuration. Rigorous output quality standards requesting correct units; significant figures are applied to ensure engineering reliability. The structured LLM agent instructions, and pseudocode of the design workflow are available in the GitHub repository, while video recordings of each agent's design generation process are included in the supplementary section. By embedding real world constraints, performance benchmarks, and full cycle problem scope, the prompt bridges theoretical modeling with practical implementation, enabling repeatable, precise, and application ready WPT designs.

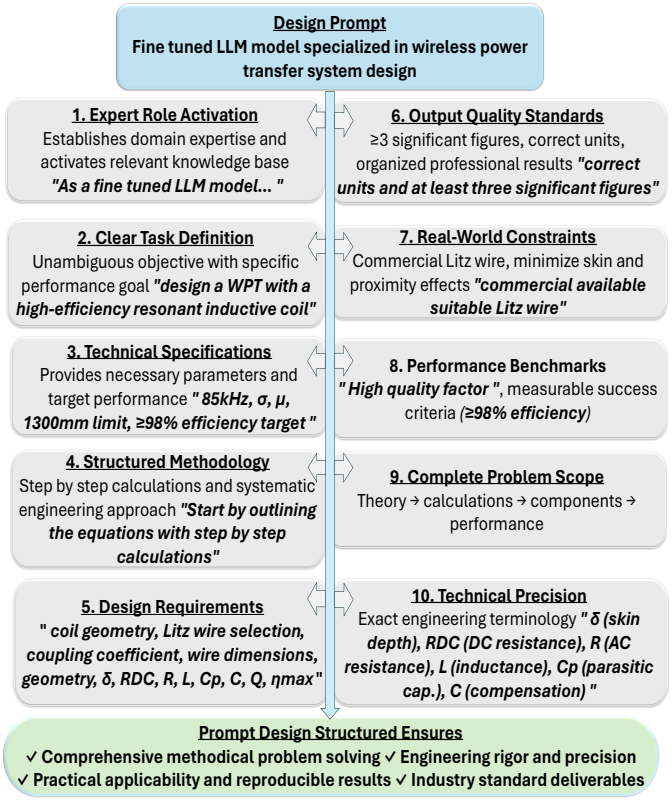


Fig. 2. Prompt structure.

To evaluate the performance of the LLM generated designs, three core metrics were introduced: design time, accuracy, and completeness. Design time saving (ΔT) quantifies the duration from the initial prompt submission to the generation of a complete design ready for simulation or fabrication, as defined in (1). Accuracy measures the degree to which the LLM generated circuit and coil parameters align with validated mathematical benchmarks, calculated using the absolute sum of percentage deviations (%Δ) as shown in (2). Where $n$denotes the total number of evaluated design parameters. The proposed accuracy metric is a signed normalized engineering deviation index rather than a bounded probabilistic measure. Positive values indicate agreement with the analytical target, while negative values indicate deviation beyond the acceptable design range. Large negative values correspond to physically inconsistent outputs and therefore indicate model instability and failure severity. Strick completeness ($S_{completeness}$)assesses whether all essential design parameters are provided within a 5% tolerance of reference values, with higher scores indicating greater consistency and reliability (3). $N_{within\ threshold}$ represent the number of predictions within the predefined accuracy threshold and N_{total} represent total number of

predictions made. The ±5% tolerance in the strict completeness index is adopted as a practical engineering acceptance margin for resonant WPT systems. In high-frequency operation, larger parameter deviations can detune resonance and reduce efficiency. Therefore, this threshold is used as an engineering consistency criterion rather than a purely statistical bound. T_{AI} represent time taken using the AI method and T_{Non-AI} is the time used compared with conventional design methods.

$$\Delta T = \left(1 - \frac{T_{AI}}{T_{Non-AI}}\right) \times 100 \quad (1)$$

$$Accuracy = 100\% - \left(\frac{\sum |\%\Delta|}{n}\right) \quad (2)$$

$$S_{completeness}\ (\%) = \left(\frac{N_{within\ threshold}}{N_{total}}\right) \times 100\% \quad (3)$$

Together, these metrics provide both quantitative and qualitative insights into the LLM's effectiveness and suitability as a design assistant in power electronics. The basic completements account the output parameters successfully generated by the LLM without accounting for the 5% tolerance.

III. Design, Modelling And simulation of WPT

A. LLM Driven Design of WPT

Table I presents the designs proposed by the finetuned LLM agents prompted to design WPT system based on prompt driven outputs. The evaluation discussed in Section II was used to select the most feasible design. Among the tested models, HFPE-4o and its variants (4o-mini, 4o-mini-high, and 4.1) demonstrated remarkable consistency in producing physically meaningful designs that closely match reference values obtained through mathematical modeling. Notably, HFPE-4o achieved a maximum theoretical efficiency (η_{max}) of 98.42% with negligible deviation in key parameters such as inductance (105.84µH), AC resistance (0.09 Ω), and resonance capacitance (33.12nF), while completing the design process in just 30 seconds representing a 99.17% reduction in time compared to conventional 1-hour modeling. With a resistive load of 10Ω, the proposed design is 150W. In contrast, HFPE-o3 and 4.1-mini exhibited significant limitations, with one producing an unphysical coupling coefficient for WPT (k ≈ 1.7) and another yielding an extreme quality factor (Q ≈ 15,453) indicative of instability and likelihood of hallucination. While HFPE-4.5 offered extremely high theoretical performance (η_{max} = 99.58%), it introduced anomalies in other components like resonance capacitance and quality factor, suggesting potential issues with model balance.

TABLE I
LLM-AI And Mathematical Modelling Design Collection

LLM Agents & Parameters	Model 1 (HFPE-4o, HFPE 4o-mini, HFPE 4o-mini-high, HFPE-4.1)	Model 2 ChatGPT 5	Model 3 (HFPE-o3)	Model 4 (HFPE-4.5)	Model 5 (HFPE 4.1-mini)	HFPE -4o	ChatGPT 5	HFPE -o3	HFPE 4o-mini	HFPE 4o-mini-high	HFPE 4.5	HFPE - 4.1	HFPE - 4.1-mini
	Mathematical Modelling Desing					LLM Driven Design							
Skin Depth δ (mm)	0.23	0.23	0.23	0.23	0.23	0.23	0.23	0.23	0.23	0.23	0.23	0.23	0.23
Number of Turns (N)	10.00	11.00	9.00	10.00	10.00	10.00	11.00	9.00	10.00	10.00	10.00	10.00	10.00
Outer Diameter Do (mm)	82.51	49.20	76.00	114.40	77.90	82.51	49.20	76.00	82.51	82.51	114.40	82.50	77.90
Trace Width w_t (mm)	3.50	1.10	3.50	3.50	3.50	3.50	1.10	3.50	3.50	3.50	3.50	3.50	3.50
Pitch Size p (mm)	3.80	1.30	3.80	3.80	3.80	3.80	1.30	3.80	3.80	3.80	3.80	3.80	3.80
Wire Length l (mm)	1300.00	1250.00	1220.00	1300.00	1300.00	1300.00	1250.00	1220.00	1300.00	1300.00	1300.00	528.00	1300.00
Litz Wire Recommended (strands × mm)	450 × 0.1	100 × 0.11	450 × 0.1	450 × 0.1	450 × 0.1	450 × 0.1	100 × 0.10	450 × 0.10	450 × 0.10	451 × 0.10	452 × 0.10	453 × 0.10	454 × 0.10
DC Resistance R_{DC} (Ω)	0.02	0.02	0.02	0.02	0.02	0.02	0.03	0.02	0.02	0.02	0.02	0.00	0.00
AC Resistance R (Ω)	0.09	0.03	0.08	0.09	0.09	0.09	0.04	0.09	0.09	0.09	0.09	0.00	0.01
Inductance L (µH)	105.84	5.42	110.72	1741.65	28.73	105.84	5.42	110.70	105.84	105.84	1.74	105.50	28.50
Parasitic Capacitance Cp (pF)	2.95	53.23	2.72	4.06	2.79	2.95	53.20	2.72	2.95	2.95	0.06	2.95	2.79
Resonance Capacitance C (nF)	33.12	646.47	31.66	2.01	122.04	33.12	647.00	31.70	33.12	33.12	2010.00	33.20	123.00
Quality Factor Q	572.63	105.26	640.48	-10538.83	166.72	572.63	78.70	692.00	572.60	572.60	103.30	15453.00	1693.00
Coupling Coefficient k	0.20	0.60	1.74	0.04	0.59	0.20	0.10	0.20	0.20	0.20	0.20	0.20	0.20
Max theoretical Efficiency ηmax (%)	98.27	0.97	99.82	99.58	0.98	98.42	77.60	98.60	98.40	98.42	90.00	90.80	99.41
Design Time (s)	3600.00	3600.00	3600.00	3600.00	3600.00	30.00	420.00	342.00	32.00	62.00	230.00	50.00	48.00

Although GPT 5 and HFPE-4o were evaluated under the same design specifications, their validated design outcomes were not equivalent. Specifically, the GPT 5 generated design exhibited an 83.2% difference in coupling coefficient during mathematical validation, indicating lower physical consistency and a higher tendency toward hallucinated outputs compared with the context finetuned HFPE-4o model. Furthermore, the total absolute percentage difference was considerably higher for GPT 5, which contributed to the observed discrepancy in theoretical efficiency. Table II summarizes the comparative

performance of the seven evaluated LLM agents. Finetuned agents, particularly the HFPE-4o variants, achieved 99 % design time reduction, good accuracy relative to analytical models, and high completeness scores (up to 92.86% completeness compared to only 35.71% with HFPE-4.1 agent). In contrast, the general purpose ChatGPT-5 and certain finetuned variants exhibited large deviations, including negative accuracy values, indicating quantitative hallucination and non-physical parameter generation. These results demonstrate substantial reliability variation across LLM architectures and underscore the importance of domain adaptation, physics informed constraints, and validation feedback loops for dependable AI assisted PE design.

TABLE II
COMPARISON OF LLM -AI AGENTS BASED ON DESIGN TIME, ACCURACY, AND COMPLETENESS SCORE.

Metric	HFPE 4o	Chat GPT 5	HFPE o3	HFPE 4o-mini	HFPE 4o-mini-high	HFPE 4.5	HFPE 4.1	HFPE 4.1-mini	Comment
Design Time Save (%)	99.17	88.33	90.50	99.11	98.28	93.61	98.61	98.67	Higher is Better
Total Absolute % Difference	0.31	8077.91	100.34	0.33	0.35	100406.33	2858.31	2.761×10^{15}	Lower is Better
Accuracy	99.98	-476.99	92.83	99.98	99.98	-7071.88	-104.17	-1.972×10^{25}	Maximum is 100%
Basic Completeness	100.00	100.00	100.00	100.00	100.00	100.00	100.00	100.00	Maximum is 100%
Strick Completeness	85.71	35.71	50.00	85.71	85.71	50.00	35.71	35.71	Higher is Better

B. Mathematical Modelling of LLM Generated Designs

To establish a performance baseline, a conventional mathematical model based on resonant inductive coupling theory was developed and used as a benchmark for evaluating the accuracy and validity of the LLM generated designs. The model computes key parameters including skin depth, DC and AC resistance, inductance, parasitic and compensation capacitance, quality factor, and theoretical maximum efficiency. Calculations are based on standard physical constants and a flat spiral coil geometry. A series-series compensated WPT configuration is considered, as shown in Fig. 3(a), where the primary and secondary inductors and compensation capacitors are tuned to achieve resonance and maximize power transfer efficiency. The corresponding circuit equations are given in (4) and (5) The source voltage is represented by V, while the terms $j\omega$ account for the reactive components in the primary and secondary circuits. Fig. 3(b) illustrates the coil geometry used as the reference for analytical modeling of the best performing LLM generated design. The mathematical modelling follows established resonant WPT design formulations reported in [4], [17] and is included here as a benchmarking layer rather than as a new contribution of this work.

$$V = (R_1 + R_s + j\omega L_1 + \frac{1}{j\omega C_1})I_1 + j\omega M I_2 \quad (4)$$

$$0 = (R_L + R_2 + j\omega L_2 + \frac{1}{j\omega C_2})I_2 + j\omega M I_1 \quad (5)$$

Where, R_s denotes the source resistance, while R_1 and R_2 represent the resistances in the primary and secondary circuits, respectively. R_L models the electrical load connected to the receiver. The currents I_1 and I_2 indicate the current flow in the primary (I_{pri}) and secondary (I_{sec}) circuits. At the resonant frequency, the inductive and capacitive reactance cancel each other, as described by (6) and (7), thereby minimizing reactive losses and maximizing power transfer efficiency.

$$V_s = (R_1 + R_s)I_1 + j\omega M I_2 \quad (6)$$

$$0 = (R_L + R_2)I_2 + j\omega M I_1 \quad (7)$$

The impedance of primary circuit coil and secondary circuit Z_2 is define by (8) and (9).

$$Z_1 = R_1 + R_s + j\omega L_1 + \frac{1}{j\omega C_1} \quad (8)$$

$$Z_2 = R_L + R_2 + j\omega L_2 + \frac{1}{j\omega C_2} \quad (9)$$

When (8) and (9) is substituted in (4) and (5) is simplified to (10) and (11). Solving for I_1 and I_2 using (12), (13), and (14) gives (15) and (16). The resonance frequency is given by (17).

$$V_s = Z_1 I_1 + j\omega M I_2 \quad (10)$$

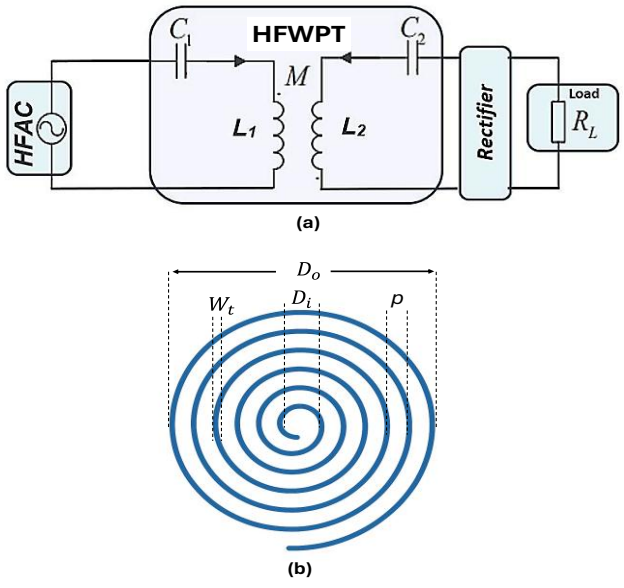


Fig. 3. (a) series-series WPT circuit diagram of HFWPT system (b) flat spiral coil geometry.

$$0 = Z_2 I_2 + j\omega M I_1 \quad (11)$$

$$I_2 = -\frac{j\omega M I_1}{Z_2} \quad (12)$$

$$V_s = Z_1 I_1 + \frac{j\omega M(-j\omega M I_1)}{Z_2} \quad (13)$$

$$V_s = I_1\left(Z_1 + \frac{\omega^2 M^2}{Z_2}\right) \quad (14)$$

$$I_1 = \frac{V_s Z_2}{Z_1 Z_2 + \omega^2 M^2} = I_{pri} \quad (15)$$

$$I_2 = -\frac{j\omega M V_s}{Z_1 Z_2 + \omega^2 M^2} = I_{sec} \quad (16)$$

$$f_o = \frac{1}{2\pi\sqrt{L_o C_o}} \quad (17)$$

For a flat spiral coil geometry reported in [18] as shown in Fig. 3(b) with outer diameter D_o given by $D_o = D_i + 2N(w_t + p)$, inner diameter D_i, wire thickness w_t , pitch p and parasitic capacitance $C_p = 0.035D_o + 0.06$, the inductance is given by (18). The resonance capacitance C_o can be obtain with (17) if the resonance frequency (f_o) is define. The coil DC resistance R_{DC}, and effective resistance R are given in (19). The Q factor and the maximum theoretical efficiency $\eta_{\max_theoretical}$ are given by (20) and (21), respectively.

$$L_o = \frac{39.37\, N_o^2\, (D_o - N_o\,(w_t+p))^2}{16D_o\, +28N_o\,(w_t+p)}\ [\mu H] \quad (18)$$

$$R = R_{DC}\frac{w_t}{4\delta}, \qquad R_{DC} = \frac{l}{\sigma\pi(w_t/2)^2},\ \delta = \frac{1}{\sqrt{\pi f_s \sigma \mu_o}} \quad (19)$$

$$Q = \frac{\omega L_{eq}}{R_{eq}} = \frac{X_{eq}}{R_{eq}} = \frac{\omega(L - C_p R^2{}_o - C_p L^2\omega^2}{R} \quad (20)$$

$$\eta_{\max_theoretical} = \frac{k^2 Q_1 Q_2}{(1+\sqrt{1+k^2 Q_1 Q_2})^2}, \text{ where } k = \frac{M}{\sqrt{L_1 L_2}} \quad (21)$$

C. Simulation and Experimental Validation

Circuit level and electromagnetic simulations were conducted to validate the feasibility of the LLM generated WPT design under practical operating conditions. Among the seven candidate designs generated by the evaluated LLM agents (Table II), the highest performing design was selected based on the benchmarking metrics defined in Section II.

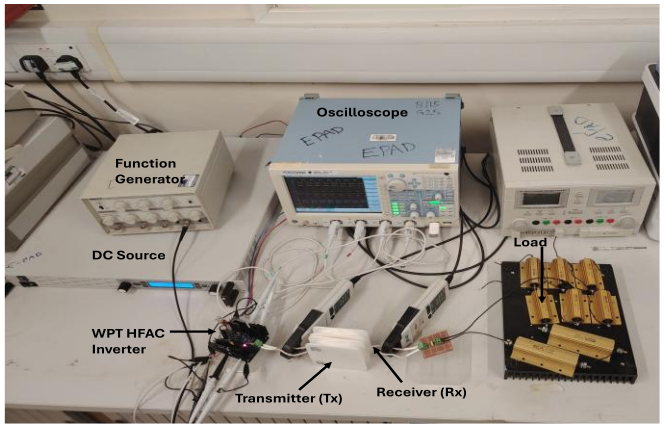


Fig. 4. Experimental set up.

Circuit level simulations were used to verify resonant operation, waveform behavior, and power transfer efficiency at the f_o of 85 kHz, while electromagnetic simulations were performed to assess magnetic field distribution and coupling characteristics of the generated coil geometry. The simulated system directly implemented the LLM generated electrical and geometric parameters, ensuring consistency between the AI output and the validation stage. The results confirm that the selected design satisfies the original specifications and is suitable for physical realization. This experimental validation confirms that the proposed LLM driven framework can reliably produce physically realizable WPT designs suitable for practical implementation. The key operating and hardware parameters of the experimental WPT setup shown in Fig. 4 are summarized in Table III.

TABLE III
HARDWARE PROTOTYPE PARAMETERS OF THE EXPERIMENTAL WPT

Parameter	Value / Component Part Number
Operating frequency (kHz)	85
Resonance Capacitors (nF)	33, SMEC333J100M1
Output power	150W
Load Resistance (Ω)	10
Main switching devices	STW62N65M5
Gate driver	IR2184SPBF
Logic stage	SN74LVC2G14DBVR
Buck regulator	LT8631IFE#PBF
Linear regulator	LM7805CT
Bulk capacitor	EEU EE2C221S, 220 µF
Coil output connector	Phoenix Contact MKDS 1,5/2-5,08 HT BK
WPT coil (strands x mm)	Litz wire 450 0.1

IV. RESULTS

Fig. 5 compares the performance of all evaluated LLM agents across four metrics: design-time reduction, strict completeness, and numerical accuracy measured by mean absolute percentage error (MAPE). As shown in Fig. 5(a) and (c), finetuned agents in the HFPE-4o agent achieved the highest computational efficiency, reducing design time by more than 99% relative to conventional manual workflows. In contrast, the general purpose ChatGPT-5 and certain non optimized models exhibited substantially lower efficiency, indicating that domain adaptation is critical for accelerating prompt-driven engineering design. Accuracy and completeness results, presented in Fig. 5(b) and (d), further highlight the advantages of finetuned models. HFPE-4o variants maintained strict completeness above 80% with MAPE values close to unity, demonstrating strong agreement with analytical benchmarks. Conversely, ChatGPT-5 and weaker finetuned variants produced large numerical deviations, with MAPE values exceeding 10^3 to10^5 %, indicative of quantitative hallucination and reduced reliability under physical constraints. Overall, the results confirm that finetuned, domain-specialized LLMs provide superior accuracy, completeness, and reproducibility compared with general-purpose models, underscoring their suitability for LLM-AI assisted design.

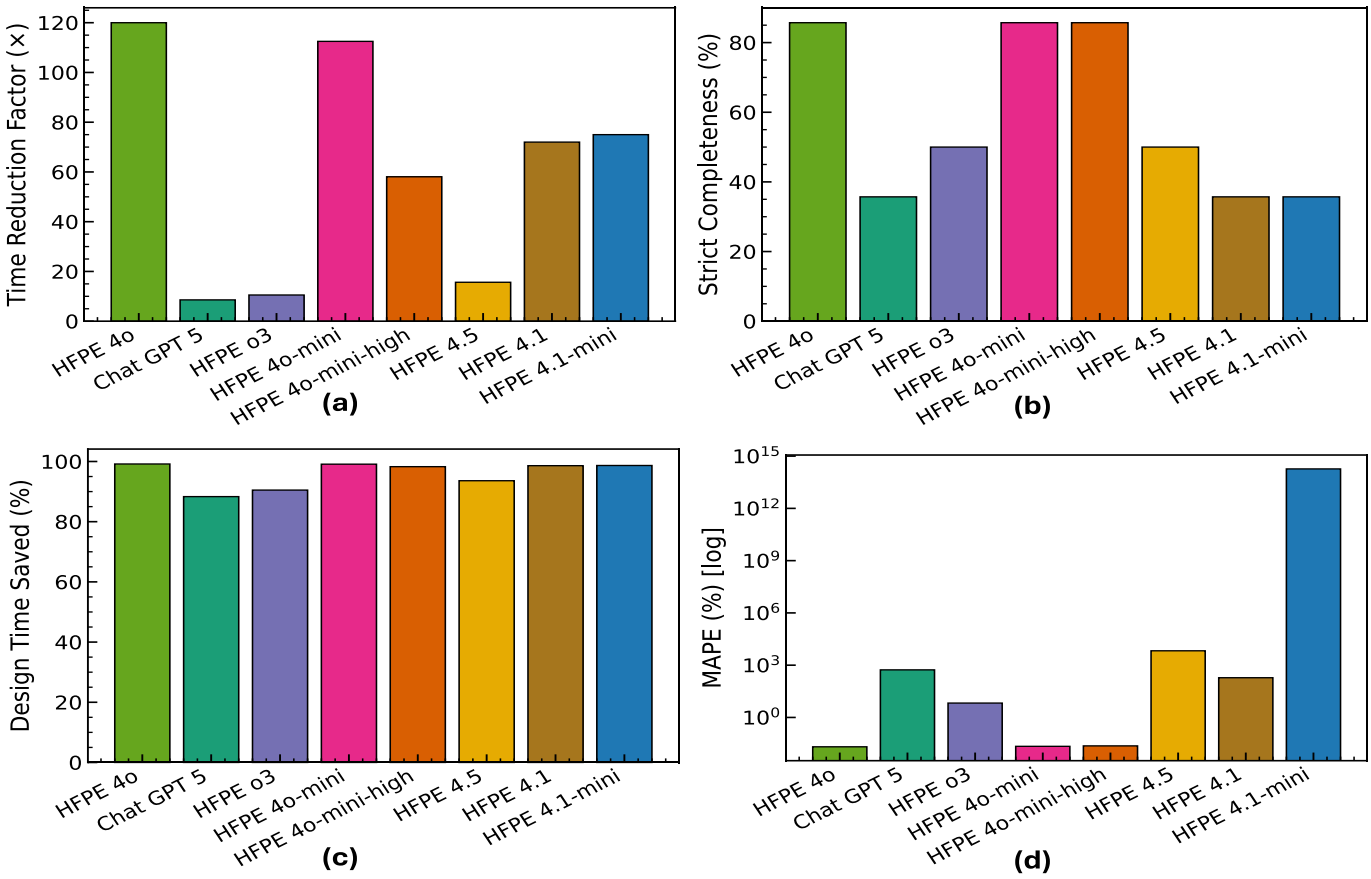


Fig. 5. Agent performance evaluation (a) time reduction factor, (b) strict completemeness, (c) design time saved (d) MAPE

Fig. 6 illustrates the time domain waveforms obtained from the PSIM simulation of the WPT system design proposed by HFPE-4o agent in Table II. The signals include the primary side current (I_{pri}), inverter output voltage (V_{pri}), secondary side current (I_{sec}), and voltage (V_{sec}). The sinusoidal shape of the primary current aligned with the square wave voltage confirms that the system operates at its resonant frequency of 85 kHz. Similarly, the clean sinusoidal waveforms on the secondary side indicate strong inductive coupling and low waveform distortion. Based on the measured RMS values, the system's power transfer efficiency was calculated to be approximately 90.2%. These results validate the feasibility and precision of the LLM generated design, highlighting the framework's effectiveness in producing a functional high-frequency WPT system.

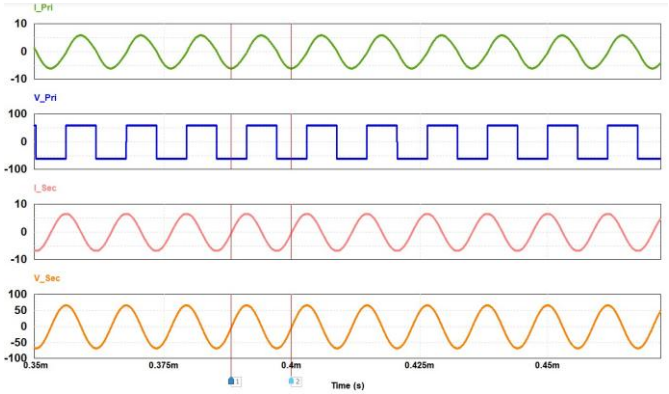


Fig. 6. PSIM simulation of WPT LLM-drven design.

To further assess operation beyond the nominal condition. Table IV present a reduced load evaluation that was conducted at lower load operating condition of 80%, 50%, and 30% relative to the rated 150 W condition. The results showed that the system remained resonant across the reduced load range, while the efficiency decreased gradually from 90.0% at full load to 79.69% at 30% light load. This behavior is consistent with expected WPT performance under reduced loading and further supports the engineering reliability of the proposed LLM generated design.

TABLE IV
RESONANCE STABILITY PERFORMANCE LOW LOAD

Output Power (W)	Load Level (%)	Efficiency (%)
150.00	100	90.00
119.92	80	86.80
74.91	50	82.64
44.96	30	79.69

Fig. 7 presents the electromagnetic field distributions of the LLM-designed WPT system obtained using ANSYS. The magnetic flux density plots in Fig. 7(a) and (b) show strong and symmetric field concentration around the primary and secondary coils, indicating effective inductive alignment and coupling. The magnetic vector field distributions in Fig. 7(c) and (d) further confirm a well directed magnetic field concentrated between the coils, with dominant mutual coupling along the axial direction.

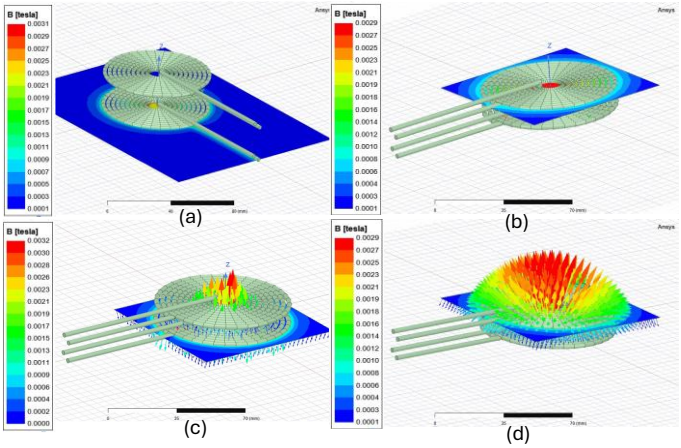


Fig. 7. Ansys simulation of the best proposed LLM drven design WPT: (a) Magnetic flux density primary coil, (b) Magnetic flux density secondary coil, (c) magnetic vector field primary coil, (d) magnetic vector field secondary coil.

These results validate the electromagnetic feasibility of the LLM generated coil parameters and confirm their suitability for efficient resonant wireless power transfer. The plot in Fig. 8 shows the variation of wireless power transfer efficiency $(\eta)$with respect to the coupling coefficient $(k)$for the best performing LLM designed system. As the value of k increases, the system efficiency rapidly rises and asymptotically approaches its theoretical maximum near 100%. Fig. 8 was obtained from ANSYS based coil level electromagnetic analysis and does not represent the exact operating point of Fig. 6. The validated design value is $k = 0.2$. This behavior highlights the effectiveness of the LLM generated coil geometry in achieving high performance under strong coupling conditions. Notably, even modest increases in k from 0.01 to 0.1 result in significant efficiency gains, reinforcing the system's suitability for tightly coupled, short range applications. This result complements Fig. 9, which presents the distance based analysis and confirms that the LLM optimized design is best deployed in scenarios where alignment and proximity can be controlled to maintain high mutual inductance.

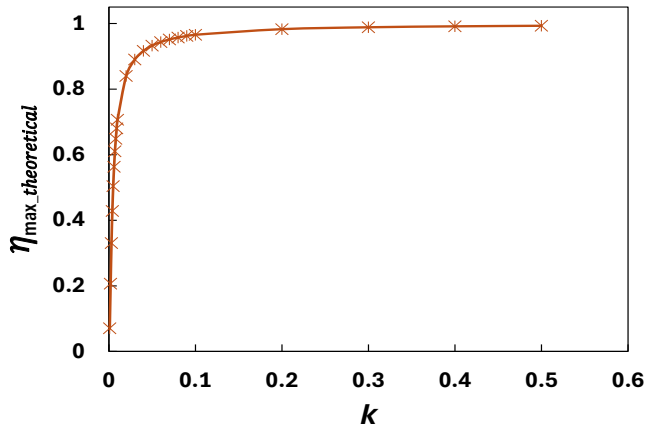


Fig. 8. WPT Efficiency (η) of the LLM generated WPT coil design as a function of coupling coefficient (k).

Fig. 9 illustrates the magnetic performance and power transfer efficiency of the best performing LLM generated WPT coil design as a function of coil separation distance. In Fig. 10 (a), the magnetic flux density (B) and magnetic field strength (H) at the receiver (Rx) drop significantly as the distance increases, whereas the transmitter (Tx) maintains a consistent field level, confirming source stability. As shown in Fig. 9 (b), this decline in Rx flux correlates with a steep reduction in wireless power transfer efficiency (η), highlighting the design's sensitivity to spatial alignment. These results suggest that the selected LLM generated coil geometry is most effective for short-range WPT applications, where coil positioning can be closely controlled. The rapid efficiency drop with increased distance reflects a design optimized for strong mutual inductance at close proximity characteristics well suited for embedded systems, charging docks, or near field power transfer. This result confirms that the LLM driven design process can produce highly efficient configurations tailored to specific operational constraints.

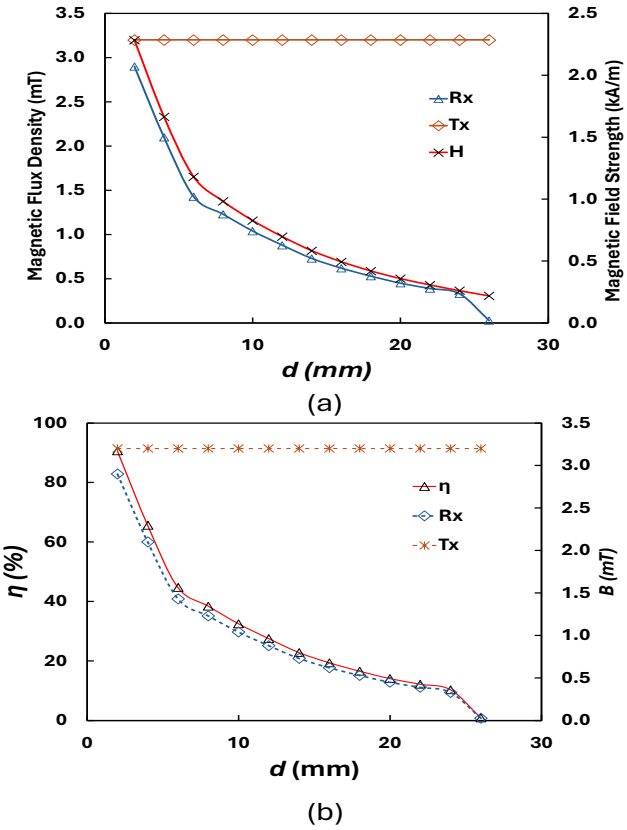


Fig. 9. Magnetic and efficiency response of the LLM driven WPT coil design versus distance: (a) Magnetic flux density and field strength variation; (b) Impact of coil separation on transmission efficiency.

Fig. 10 presents the experimentally measured voltage waveforms across each switch in the square wave inverter, operating at 85 kHz. This setup was implemented to replicate the switching behavior simulated in PSIM and ensure consistency throughout the AI driven WPT design pipeline. The clear square voltage profiles across all switches confirm proper full bridge operation and validate that the inverter functions using square waves similar to the simulation. The close alignment with the simulated waveforms reinforces the reliability of the LLM generated parameters and supports their applicability in practical hardware implementations.



Fig. 10. Measured voltage waveforms across each inverter switch in the experimental square-wave WPT setup.

Fig. 11 presents the measured oscilloscope waveforms of the wireless power transfer system implemented using the best-performing LLM-generated design. The switching voltages of the two inverter legs and the corresponding primary coil current are shown. The inverter operates at approximately 85.2 kHz, closely matching the LLM-predicted resonant frequency. The near sinusoidal coil current confirms resonant operation and stable power transfer, validating the practical accuracy and physical feasibility of the LLM-guided design.

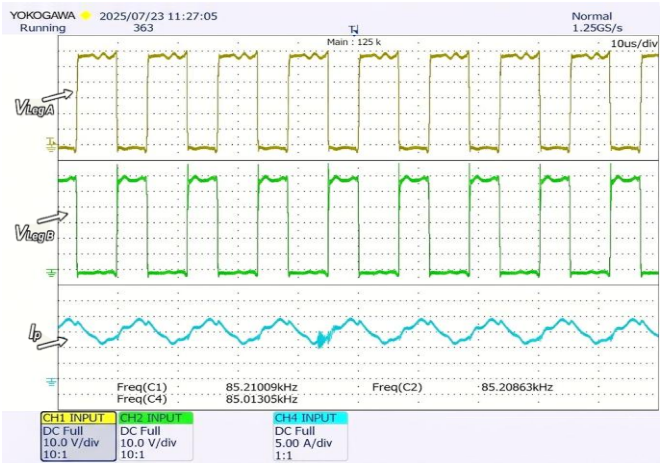


Fig. 11. Experimental waveforms of the LLM generated WPT system: inverter leg switching voltages and primary coil current at an operating frequency of 85.2 kHz s(60 V input, 10 Ω load).

Fig. 12 compares the simulated and experimental efficiencies of the LLM designed WPT system as a function of coil separation. While the experimental prototype achieves a peak efficiency of 81% compared to 90% in simulation, both curves exhibit the same decay trend with increasing distance, validating the predictive capability of the LLM-AI assisted design. To highlight the similarity in performance trends, the efficiencies are also normalized to their respective maxima. This normalization removes the influence of absolute value differences and emphasizes the consistent degradation profile across both models, demonstrating that the simulation accurately captures the coupling behavior despite practical losses and uncertainties not fully captured in simplified analytical or circuit level models, including inverter switching and conduction losses, capacitor ESR, AC copper losses due to skin and proximity effects, parasitic resistance, fabrication tolerances, and alignment deviations.

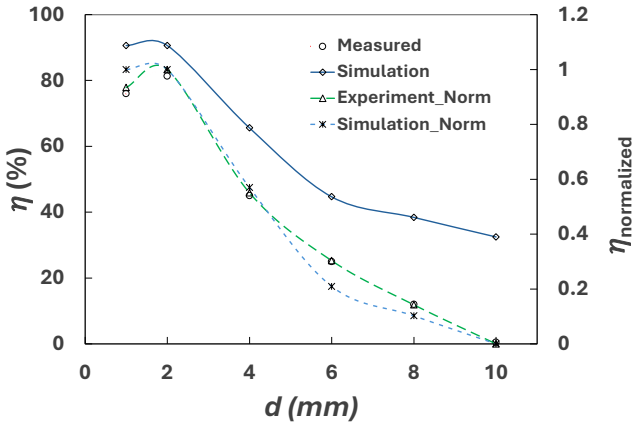


Fig. 12. Measured and simulated WPT efficiency versus coil separation, with normalized comparison.

An overload test was conducted using a 6.67Ω resistive load, corresponding to a 50 % increase in output power relative to the nominal 10Ω operating condition, to evaluate the system's electrical and thermal robustness under stressed operation. Such testing is essential for assessing reliability, safety margins, and failure thresholds in practical WPT applications subject to dynamic loading. Fig. 13 illustrates the system response under overload conditions. The inverter output voltages exhibit increased high frequency switching distortion, while the primary coil current shows pronounced waveform distortion and a frequency shift from the nominal 85 kHz to approximately 97.95 kHz. This deviation is attributed to elevated current stress, parasitic heating, and thermally induced parameter variations in the resonant tank and gate drive circuitry. The observed resonance detuning and waveform irregularities indicate degraded operating stability and the onset of potential HFAC inverter failure, providing critical insight into safe operating limits and thermal constraints of the LLM generated design.

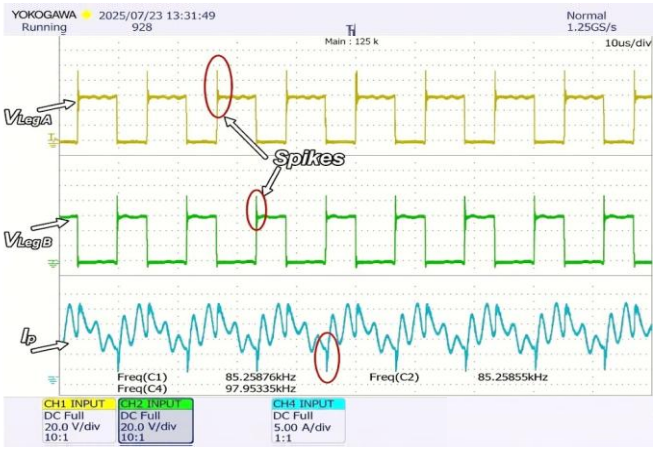


Fig. 13. Electrical response of the WPT system under overload conditions with a 6.67 Ω load.

Fig. 14 presents the thermal response of the WPT system under nominal and overload operating conditions. Under nominal conditions, the coil temperature remained at 35.8 °C, while the gate driver IC reached 74.7 °C, both within acceptable operating limits. Under overload conditions, the resonance capacitor temperature increased to 75.8 °C and remained stable;

however, the gate driver IC experienced a rapid temperature rise from 87.2 °C to 151 °C, resulting in component failure. These results indicate that while the LLM generated coil design exhibits strong thermal resilience, the HFAC driving circuitry represents the dominant thermal bottleneck. The thermal measurements therefore establish practical safety margins and identify critical components governing system reliability under high stress operation. In addition, the LLM capability to integrate thermal data needs to be explore in future research. Experimental light load testing was not performed because the overload test caused failure of the resonance capacitor in the prototype, preventing further safe operation of the same hardware configuration. Further experimental validation under light load conditions will be considered in future work.

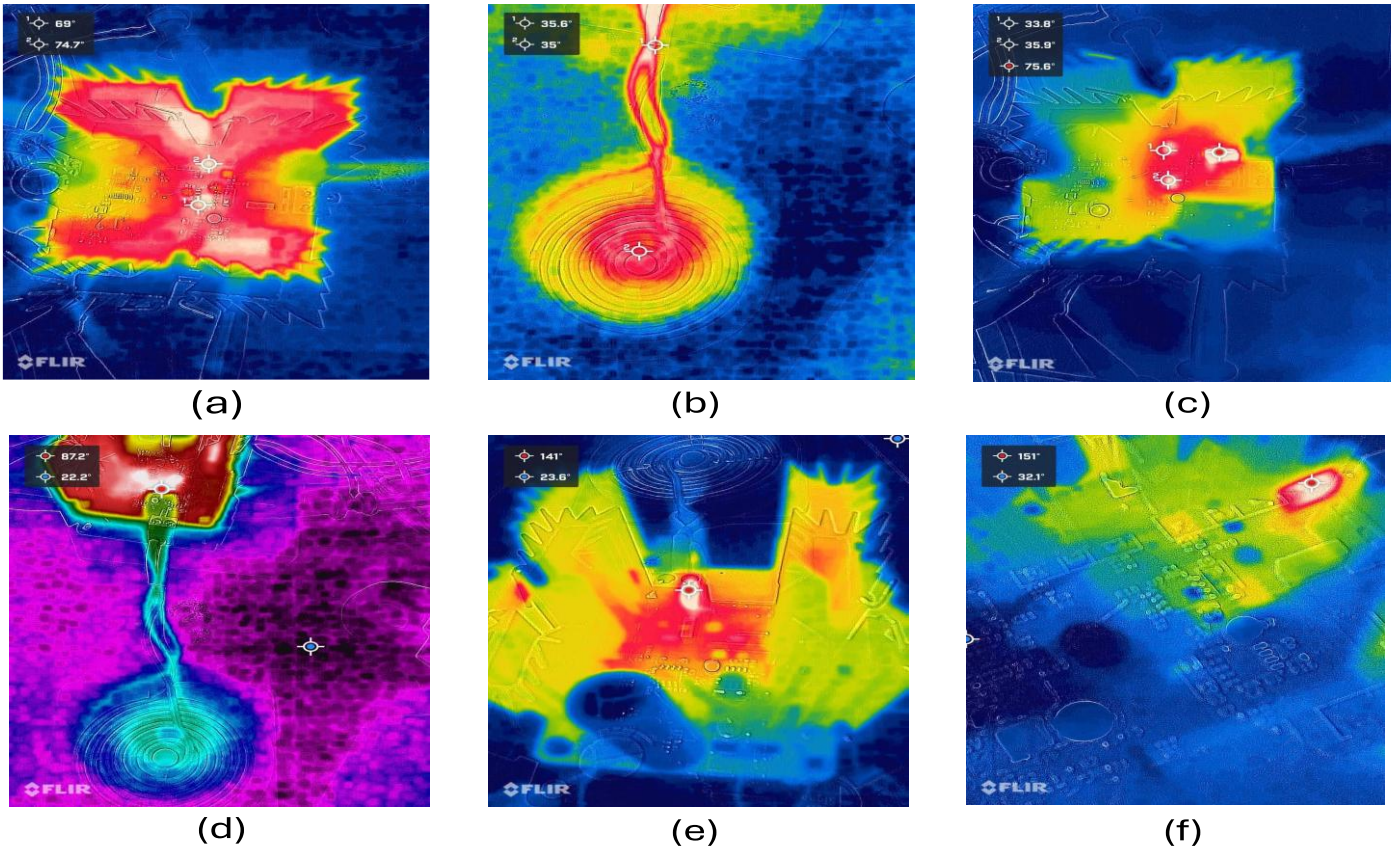


Fig. 15. Thermal images of the LLM generated WPT system under nominal and overload operating conditions: (a), (b) normal operation at 60 V input and 10 Ω load; (c) to (f) progressive thermal stress under overload at 60 V input and 6.67 Ω load.

To distinguish the design stage discrepancy from the implementation stage loss, the efficiency progression of the best HFPE-4o design was examined across multiple validation levels. The best performing large model agent based on evaluation matrix proposed a maximum theoretical efficiency of 98.42%, while mathematical validation gave 98.27%, corresponding to a discrepancy of 0.15% at the design stage. The PSIM nominal simulation yielded 90.20%, representing a reduction of 8.07% relative to the mathematically validated value, while the ANSYS electromagnetic analysis showed a maximum coupling efficiency of 90.625% at 2 mm separation, corresponding to a reduction of 7.65%. Finally, the experimental prototype achieved a peak efficiency of 81.00%, corresponding to a further reduction of 9.20% relative to PSIM. This progression indicates that the discrepancy introduced by the large model is limited, whereas the larger efficiency reductions arise mainly during simulation and physical experimental implementation.

V. Conclusion

This paper presented an LLM AI driven, agentic framework for the automated design of resonant inductive WPT systems using large language models. The proposed approach enables the rapid generation of complete WPT designs, including coil geometry, component values, and circuit configuration, within seconds. Simulation and experimental validation confirmed that the LLM generated design is physically feasible and achieves competitive performance under nominal operating conditions. Robustness evaluation under overload conditions revealed thermally induced resonance detuning and failure in the gate drive circuitry, while the coil remained within safe operating limits. These results highlight both the strengths and current limitations of LLM based design automation: while effective for generating functional electromagnetic and circuit level designs, present day LLMs do not inherently account for thermal stress, frequency drift, or overload behavior. Consequently, simulation and experimental validation remain essential for ensuring safe and reliable operation. Overall, this work demonstrates the potential of generative AI to significantly accelerate early stage PE design and enable rapid prototyping. Future integration of optimization algorithms, thermal modeling, and closed loop simulation feedback is expected to further enhance the reliability and applicability of LLM driven design frameworks. As larger, validated datasets from power electronics systems become available, LLMs are anticipated to evolve into effective co design assistants, supporting faster development cycles and

improved design exploration across a wide range of power electronic applications.

Extension of the proposed framework to higher order compensation topologies such as LCC-S and LCC-LCC would require the incorporation of topology specific constraint modules, including additional resonant branch relationships, inductor and capacitor design rules, reflected impedance constraints, current and voltage stress limits, and switching condition constraints. By updating these structured constraint blocks, together with operating and mechanical constraints, within the LLM design loop, the same benchmarking methodology can be extended to more complex WPT topologies without changing the overall framework logic. Future work will further consider the integration of optimization algorithms, closed-loop simulation feedback, and validation across a wider range of WPT topologies and power levels. Although this study focused on a single resonant WPT case, the proposed benchmarking framework and evaluation metrics are topology agnostic and can be applied to other high-frequency power electronics systems, including resonant converters and inverter based energy architectures. Overall, this work establishes a foundation for reliable, data driven LLM-assisted design in high-frequency power electronics.

SUPPLEMENTARY

Videos demonstrating each LLM agent, and the agent instructions, pseudocode, workflow will be available through ttps://github.com/Khalifa44432/Engineering-Viability-of-LLM-Based-AI-Design

REFERENCES

[1] F. Salomez *et al.*, 'State of the Art of Research towards Sustainable Power Electronics', *Sustainability*, vol. 16, no. 5, p. 2221, Mar. 2024, doi: 10.3390/su16052221.

[2] C. Thingom, A. S. M. Antony, B. Trinadha, R. V, S. S. Kumar, and A. Sharma, 'AI-Assisted Design of Power Electronic Circuits', in *2025 Global Conference in Emerging Technology (GINOTECH)*, IEEE, May 2025, pp. 1–5. doi: 10.1109/GINOTECH63460.2025.11076945.

[3] S. Krishnamoorthy, 'Leveraging Generative AI for Platform Hardware Design Automation - Learnings and Recommendations', in *Proceedings - International Symposium on Quality Electronic Design, ISQED*, IEEE Computer Society, 2025. doi: 10.1109/ISQED65160.2025.11014418.

[4] K. A. Ibrahim, P. C.-K. Luk, Z. Luo, S. Y. Ng, and L. Harrison, 'Revolutionizing power electronics design through large language models: Applications and future directions', *Computers and Electrical Engineering*, vol. 123, p. 110248, Apr. 2025, doi: 10.1016/j.compeleceng.2025.110248.

[5] J. Li, H. Yan, R. Ji, X. Liang, and S. Sam Ge, 'Finite-Time Event-Triggered Fuzzy Adaptive Prescribed Force Loading Control of Electrohydraulic Load Simulator', *IEEE Transactions on Industrial Electronics*, vol. 72, no. 12, pp. 14018–14027, Dec. 2025, doi: 10.1109/TIE.2025.3579064.

[6] P. S. Subudhi and S. Krithiga, 'Wireless Power Transfer Topologies used for Static and Dynamic Charging of EV Battery: A Review', 2020. doi: 10.1515/ijeeps-2019-0151.

[7] R. Qin, J. Li, J. Sun, and D. Costinett, 'Shielding Design for High-Frequency Wireless Power Transfer System for EV Charging With Self-Resonant Coils', *IEEE Trans. Power Electron.*, vol. 38, no. 6, 2023, doi: 10.1109/TPEL.2023.3251990.

[8] H. Li, X. Ji, X. Kou, H. Wang, and M. Fu, 'Low-Radiation Multiple-Coil Wireless Charger Using Detuned Compensation', *IEEE Transactions on Industrial Electronics*, vol. 72, no. 12, pp. 12666–12674, Dec. 2025, doi: 10.1109/TIE.2025.3566720.

[9] T. Lagier *et al.*, 'How Good are the Design Tools in Power Electronics?', in *2020 22nd European Conference on Power Electronics and Applications (EPE'20 ECCE Europe)*, IEEE, Sep. 2020, p. P.1-P.12. doi: 10.23919/EPE20ECCEEurope43536.2020.9215942.

[10] J. Jose, J. P. Therattil, T. Jarin, B. Deepanraj, and M. Sumbwanyambe, 'Intelligent Circuit Optimization for a Wireless Power Transfer System Based on L2CL-LCL Compensation', in *International Conference on Distributed Computing and Optimization Techniques, ICDCOT 2024*, Institute of Electrical and Electronics Engineers Inc., 2024. doi: 10.1109/ICDCOT61034.2024.10515425.

[11] A. J. Marques Cardoso, 'Power Electronics Design Methods and Automation in the Digital Era: Evolution of Design Automation Tools', *IEEE Power Electronics Magazine*, vol. 7, no. 2, 2020, doi: 10.1109/MPEL.2020.2988077.

[12] T. Tigerprints and Y. Li, 'VIRTUAL PROTOTYPING OF PEBB BASED POWER ELECTRONICS VIRTUAL PROTOTYPING OF PEBB BASED POWER ELECTRONICS SYSTEM FOR GROUND VEHICLES SYSTEM FOR GROUND VEHICLES', Clemson University, Clemson, South Calrolina, 2023. Accessed: May 29, 2024. [Online]. Available: https://tigerprints.clemson.edu/cgi/viewcontent.cgi?article=5120&context=all_theses

[13] N. Mariun, B. Omrane, I. Aris, S. Mahmoud, and T. Soib, 'Power electronics design aid system, a knowledge-based approach', in *Proceedings of the International Conference on Power Electronics and Drive Systems*, 2003. doi: 10.1109/PEDS.2003.1283112.

[14] M. Petkovski and M. Kostov, 'Model Based Design and Hardware in the Loop Testing in Power Electronics Courses', *TEM Journal*, vol. 1, no. 4, pp. 292–296, 2012, Accessed: May 29, 2024. [Online]. Available: https://eprints.uklo.edu.mk/id/eprint/1322

[15] X. Li, G. Tian, and Y. Cui, 'Task Guided Multimodal Object Search for Service Robots via Reinforcement Learning', *IEEE Transactions on Industrial Electronics*, vol. 72, no. 12, pp. 13786–13795, Dec. 2025, doi: 10.1109/TIE.2025.3584983.

[16] T. Dragicevic, P. Wheeler, and F. Blaabjerg, 'Artificial Intelligence Aided Automated Design for Reliability of Power Electronic Systems', *IEEE Trans. Power Electron.*, vol. 34, no. 8, pp. 7161–7171, Aug. 2019, doi: 10.1109/TPEL.2018.2883947.

[17] M. Kavitha, P. B. Bobba, and D. Prasad, 'Comprehensive mathematical modelling and experimental analysis of a wireless power transfer system for neighborhood electric vehicles', in *2015 IEEE International WIE Conference on Electrical and Computer Engineering (WIECON-ECE)*, IEEE, Dec. 2015, pp. 275–279. doi: 10.1109/WIECON-ECE.2015.7443916.

[18] M. Kim, M. Jeong, M. Cardone, and J. Choi, 'Design of a Spiral Coil for High-Frequency Wireless Power Transfer Systems Using Machine Learning', *IEEE Journal of Emerging and Selected Topics in Industrial Electronics*, vol. 5, no. 1, 2024, doi: 10.1109/JESTIE.2023.3317797.



KHALIFA ALIYU IBRAHIM (member, IEEE) received the B.Sc. degree in Physics (First Class) from Kaduna State University, Nigeria, in 2016, and the two M.Sc. degrees in Energy, Thermal and Power system from Cranfield University, U.K., in 2021 and 2022. He is currently a Research Assistant and Ph.D. researcher at Cranfield University. His research focuses on LLM AI-driven high frequency power electronics design.



PATRICK CHI-KWONG LUK (Senior Member, IEEE) received the Higher Diploma from The Hong Kong Polytechnic University in 1983, the M.Phil. degree from The University of Sheffield in 1989, and the Ph.D. degree from the University of South Wales in 1992, all in electrical engineering. He joined Cranfield University, U.K., in 2002, where he is Chair Professor of Electrical Engineering. He has published

over 240 papers in power electronics and motor drives and has served as Chairman of the IEEE U.K.&I Power Electronics Chapter, Associate Editor of the IEEE Transactions on Power Electronics, and Distinguished Lecturer for the IEEE Vehicular Technology Society. His research interests include electrical drives, electronics, and energy conversion systems.



ZHEN-HUA LUO received the Ph.D. degree in Materials Science and Engineering from the University of New South Wales, Australia, in 2011. He is currently a Reader in Energy Storage and Harvesting at Cranfield University, U.K. His research focuses on renewable energy conversion, energy systems and hydrogen generation. He is a recipient of the 2024 U.K. Universities Award for Excellence in Hydrogen Research and Innovation.



SENGN YIM NG, received the Ph.D. degree in Electrical and Electronic Engineering from Cranfield University, U.K. He has over 20 years of experience in high-frequency power conversion for industrial and transportation systems. He leads advanced research in embedded power distribution and serves as Industrial Supervisor for Cranfield's Ph.D. program in power electronics.



LEE HARRISON, is an entrepreneur with over 30 years of experience in power conversion and system architecture. He has collaborated with major technology companies and co-authored the industry standard 80+ power supply specification. He holds multiple patents and a Red Dot Design Award for innovations in high-efficiency AC–DC power system.



https://dspace.org/

Benchmarking the engineering reliability of LLM-based design for resonant wireless power transfer systems

Ibrahim, Khalifa Aliyu; Luk, Patrick Chi-Kwong; Luo, Zhenhua; Ng, Seng Yim; Harrison, Lee

2026-12-31
Institute of Electrical and Electronics Engineers (IEEE)
https://doi.org/10.1109/tie.2026.3695234
Ibrahim KA, Luk PC-K, Luo Z, et al., (2026) Benchmarking the engineering reliability of LLM-based design for resonant wireless power transfer systems. IEEE Transactions on Industrial Electronics, available online 16 June 2026

Downloaded from a DSpace repository. https://dspace.org/